

# ON THE SPECTRAL GROWTH OF THE POLAR REPRESENTATION OF COMMUNICATION SIGNALS

Bin Yang

Institute of Signal Processing and System Theory, University of Stuttgart, Germany

## ABSTRACT

The traditional modulator in digital communication systems is the quadrature (IQ) modulator using the Cartesian representation of a complex baseband signal. In the last years, the polar transmitter has been becoming an attractive alternative due to its significantly increased energy efficiency. It uses a polar representation of the baseband signal before transmission. The result of the changed signal representation is an internal spectral growth of the polar signals whose understanding is fundamental for the design of modern polar transmitters. This paper gives a mathematical analysis of the spectral growth of the polar signals.

**Index Terms**— signal representation, polar transmitter, polar signals, spectral growth

## 1. INTRODUCTION

Modern communication systems often suffer from a large peak-to-average ratio (PAR). In a traditional Cartesian transmitter doing an upconversion of the inphase (I) and quadrature (Q) component of the complex baseband signal, the power amplifier (PA) is requested to operate in a highly linear mode. Due to the large PAR value, a large power back-off in the PA is necessary, resulting in a lower energy efficiency.

Kahn proposed an envelope elimination and restoration technique in [1]. Instead of mixing  $(i, q)$  by an IQ-modulator, the amplitude  $r$  and phase  $\theta$  of the complex baseband signal are extracted from the IQ-signal, processed separately, and recombined at the PA. In this case, there is no need for a highly linear PA. The PA rather operates in the switch mode with a significantly increased energy efficiency and reduces the power consumption of the transmitter. Today this concept is known as polar transmitter [2]. It is a promising transmitter architecture to meet both the spectral and energy efficiency requirement. The amplitude  $r$ , phase  $\theta$ , and constant-envelope phase-modulated signal  $e^{j\theta}$  are called polar transmitter signals or simply polar signals.

As a result of the changed signal representation inside the modulator, a spectral growth has been observed: the polar signals  $r, \theta$  have a much wider spectrum than the corresponding Cartesian signals  $i, q$ . As a rule of thumb, a factor 10 of spectral growth for the phase and a factor of 2–4 for the amplitude is often cited from measurements and simulations [3, 4, 5]. There are some heuristic explanations for the spectral growth, but there have been no theoretical studies yet.

This is prohibitive for the system and circuit designers of polar transmitters. They need to understand why and how does the bandwidth of the polar signals increase in order to design the modulator circuits properly.

This paper gives a theoretical analysis of the spectral growth of the polar representation of communication signals. The analysis is done by assuming a complex-Gaussian baseband signal and deriving its statistical properties (pdf, covariance function, spectrum) in the polar domain from those in the Cartesian domain.

The paper is organized as follows: Section 2 introduces the basic polar transmitter architecture. Section 3 discusses the exact model and a simplified Gaussian model of the baseband signal. Section 4 performs an analytic study of the spectral growth of the polar signals under the simplified signal model. The results are verified with simulations in section 5.

## 2. POLAR TRANSMITTER AND POLAR SIGNALS

Fig. 1 shows the basic architecture of a polar transmitter. The baseband processor generates a sequence of discrete-time complex symbols  $a_n \in \mathbb{C}$ . The continuous-time *pulse shaping filter*  $g(t) \in \mathbb{R}$  converts the sequence of complex symbols  $a_n$  to an analog complex-valued baseband signal

$$s(t) = \sum_{n=-\infty}^{\infty} a_n g(t - nT_{\text{sym}}) = i(t) + jq(t) = r(t)e^{j\theta(t)} = r(t)m(t) \quad (1)$$

where  $T_{\text{sym}}$  is the symbol period. The Fourier transform  $G(\omega) = \mathcal{F}(g(t))$  of  $g(t)$  determines the spectrum and bandwidth of  $s(t)$ . The *inphase*  $i(t) = \text{Re}(s(t))$  and *quadrature* component  $q(t) = \text{Im}(s(t))$  represent the Cartesian coordinates of  $s(t)$  and are called IQ- or *Cartesian signals*. The *polar signals* are

$$\begin{aligned} r(t) &= |s(t)| = \sqrt{i^2(t) + q^2(t)} \geq 0, \\ \theta(t) &= \arg(s(t)) \in [-\pi, \pi), \\ m(t) &= s(t)/|s(t)| = e^{j\theta(t)} \in \mathbb{C}. \end{aligned} \quad (2)$$

$r(t)$  is the *amplitude* or *envelope*.  $\theta(t)$  is the *phase* component of  $s(t)$ .  $m(t)$  is the complex-valued *constant-envelope phase-modulated signal* with  $|m(t)| = 1$ . The conversion from the Cartesian domain  $(i, q)$  to the polar domain  $(r, \theta)$  is typically done by a coordinate rotation digital computer (CORDIC)

[9, 10]. The complex baseband signal can then be written as  $s(t) = r(t)m(t)$ . This multiplication corresponds to the recombination in the PA in a polar transmitter. The transmitted RF signal is

$$\text{Re}(s(t)e^{j\omega_c t}) = r(t) \cos(\omega_c t + \theta(t)) \quad (3)$$

where  $\omega_c$  is the carrier frequency. Since the effect of the carrier  $\omega_c$  is well known (shifts a spectrum from baseband to passband), this paper studies the spectral growth of the baseband polar signals  $r(t), \theta(t), m(t)$  only.

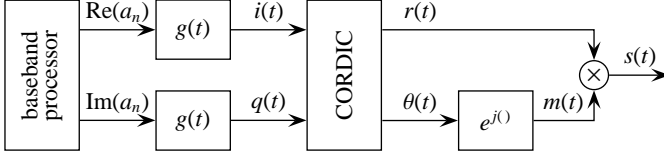


Fig. 1. Baseband representation of a polar transmitter

### 3. SIGNAL MODEL

#### 3.1. The pdf approach

In a Cartesian transmitter, the baseband signal  $s = i + jq$  is a linear function of  $i, q$ . Hence the spectrum of  $s$  is simply the sum of the spectra of  $i, q$  if  $i$  and  $q$  are uncorrelated:

$$C_{ss}(\omega) = C_{ii}(\omega) + C_{qq}(\omega). \quad (4)$$

Often,  $C_{ii}(\omega) = C_{qq}(\omega)$  and thus  $C_{ss}(\omega) = 2C_{ii}(\omega)$ . This means, there is no difference in the spectral shape between the baseband signal  $s$  and its Cartesian components  $i, q$ .

This is not the case for the polar representation  $r, \theta, m$  of  $s$  because they are *nonlinear* functions of  $i, q$ . Therefore, the 2nd order moments (covariance function and spectrum) of  $r, \theta, m$  do not only depend on the 2nd order moments of  $i, q$ , but rather on their probability density function (pdf). If only the spectra of  $i, q$  are known but not their distribution, the spectra of  $r, \theta, m$  cannot be determined. This is also true in the opposite direction.

In order to predict the spectral growth of the polar signals, one has to follow the pdf approach in Fig. 2. Consider two baseband samples  $s_k = s(t_k) = i_k + jq_k = r_k e^{j\theta_k} = r_k m_k, k = 1, 2$  at the time instants  $t_1, t_2$  with the time lag  $t = t_1 - t_2$ . The starting point of the analysis is the joint pdf  $p(i_1, i_2, q_1, q_2; t)$  of the Cartesian components  $i_1, i_2, q_1, q_2$ . From that, one can calculate the joint pdf  $p(r_1, r_2, \theta_1, \theta_2; t)$  of the polar components  $r_1, r_2, \theta_1, \theta_2$  and then their bivariate pdf  $p(r_1, r_2; t), p(\theta_1, \theta_2; t)$ , covariance functions  $c_{rr}(t), c_{\theta\theta}(t), c_{mm}(t)$ , and finally the corresponding spectra  $C_{rr}(\omega), C_{\theta\theta}(\omega), C_{mm}(\omega)$ . There is no shortcut between the Cartesian spectra  $C_{ii}(\omega), C_{qq}(\omega)$  and polar spectra  $C_{rr}(\omega), C_{\theta\theta}(\omega), C_{mm}(\omega)$ .

#### 3.2. The exact signal model

To determine the joint pdf  $p(r_1, r_2, \theta_1, \theta_2; t)$ , one needs to consider the signal model for  $s(t)$ . Recall the *exact model* of the

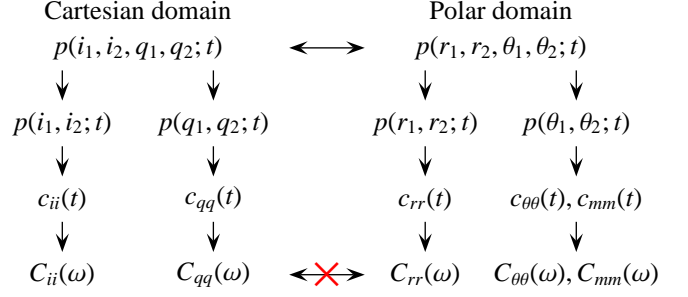


Fig. 2. The pdf approach to compute the spectra in the Cartesian and polar domain

baseband signal  $s(t)$  in Eq. (1).  $a_n \in \mathbb{C}$  is a sequence of i.i.d. random variables with zero mean and variance  $\sigma_a^2$ . The pdf of  $a_n$  depends on the constellation diagram of the modulation and on the optional IFFT in OFDM systems. In general, the exact pdf of the continuous-time baseband signal  $s(t)$  is unknown and difficult to determine. But it is easy to show that

- $s(t)$  has zero mean and the covariance function

$$c_{ss}(t + \tau, \tau) = \sigma_a^2 \sum_{n=-\infty}^{\infty} g(t + \tau - nT_{\text{sym}})g(\tau - nT_{\text{sym}}) \quad (5)$$

where  $t$  is the time lag and  $\tau$  the absolute time instant.

- $s(t)$  is *not* stationary because  $c_{ss}(t + \tau, \tau)$  depends both on the time lag  $t$  and the absolute time instant  $\tau$ . To be more precise,  $s(t)$  is *cyclostationary* [11, 12] and  $c_{ss}(t + \tau, \tau)$  is periodic in  $\tau$  with the period  $T_{\text{sym}}$ . In theory,  $s(t)$  has no spectrum as its spectral power distribution changes in  $\tau$  periodically.
- In [11], the *average covariance function*

$$\bar{c}_{ss}(t) = \frac{1}{T_{\text{sym}}} \int_0^{T_{\text{sym}}} c_{ss}(t + \tau, \tau) d\tau = \frac{\sigma_a^2}{T_{\text{sym}}} \int_{-\infty}^{\infty} g(t + \tau)g(\tau) d\tau \quad (6)$$

and the *average covariance spectrum*

$$\bar{C}_{ss}(\omega) = \mathcal{F}(\bar{c}_{ss}(t)) = \frac{\sigma_a^2}{T_{\text{sym}}} |G(\omega)|^2 \quad (7)$$

are proposed to describe the average correlation and spectral properties of a cyclostationary signal. Clearly, the pulse shaping filter  $g(t)$  determines the spectrum and bandwidth of  $s(t)$ .

- In general, the real and imaginary part of  $a_n$  are dependent (e.g. in a phase modulation with  $|a_n| = 1$ ), but they are uncorrelated due to rotation-symmetric constellation points  $a_n$ . Since  $a_m$  and  $a_n$  are independent  $\forall m \neq n$ ,  $i(t_1)$  and  $q(t_2)$  are also uncorrelated  $\forall t_1, t_2$ .

#### 3.3. A simplified signal model

Unfortunately, the above exact signal model is not suitable for an analytic study of the polar signals because there is no analytic expression for the joint pdf of  $s(t)$ . Below three

model approximations are made leading to a *simplified Gaussian model* for  $s(t)$  which allows an analytical study of  $s(t)$  in the polar domain:

A1) In the non-OFDM case, each value of  $s(t)$  is a superposition of several independent symbols  $a_n$  because the pulse shaping filter  $g(t)$  has typically a length of several symbol periods. In the OFDM case, each  $a_n$  is the output of an IFFT, i.e. a linear combination of an even larger number of independent symbols. According to the central limit theorem [12],  $s(t)$  is approximately Gaussian distributed with zero mean.

A2) In the exact signal model,  $i(t_1)$  and  $q(t_2)$  are uncorrelated. Since  $s(t)$  is Gaussian in the simplified model,  $i(t_1)$  and  $q(t_2)$  are also independent with identical variances. This means,  $s(t)$  is circular complex Gaussian.

A3)  $s(t)$  is assumed to be stationary with the covariance function  $c_{ss}(t) = \frac{\sigma_a^2}{T_{\text{sym}}} \int_{-\infty}^{\infty} g(t+\tau)g(\tau)d\tau$  and the spectrum  $C_{ss}(\omega) = \frac{\sigma_a^2}{T_{\text{sym}}} |G(\omega)|^2$  as in Eq. (6) and (7).

According to these assumptions,  $s(t)$  can be approximated by a stationary, zero-mean, and circular complex Gaussian signal whose statistical properties are completely described by the 2nd order moment of  $s(t)$ , i.e. its spectrum. Due to this distribution assumption, it is now possible to compute the spectra of the polar signals  $r(t)$ ,  $\theta(t)$ ,  $m(t)$  from those of the Cartesian signals  $i(t)$ ,  $q(t)$  by using the pdf approach in Fig. 2. Section 5 shows later how sensitive are the results with respect to this model approximation.

#### 4. SPECTRAL GROWTH IN THE POLAR DOMAIN

Let  $s_k = s(t_k) = i_k + jq_k = r_k e^{j\theta_k} = r_k m_k$ ,  $k = 1, 2$  be two random samples of  $s(t)$  at any two instants  $t_1, t_2$ . According to the simplified circular complex Gaussian model, the real random vector  $[i_1, i_2, q_1, q_2]^T$  is  $N(\underline{0}, \mathbf{C})$  distributed with the covariance matrix

$$\mathbf{C} = \begin{bmatrix} \sigma^2 & \rho\sigma^2 & 0 & 0 \\ \rho\sigma^2 & \sigma^2 & 0 & 0 \\ 0 & 0 & \sigma^2 & \rho\sigma^2 \\ 0 & 0 & \rho\sigma^2 & \sigma^2 \end{bmatrix}. \quad (8)$$

$\sigma^2$  is the identical variance of  $i(t)$ ,  $q(t)$  and  $\rho = \rho(t)$  is the normalized correlation coefficient between  $i(t_1)$ ,  $i(t_2)$  as well as  $q(t_1)$ ,  $q(t_2)$  with the time lag  $t = t_1 - t_2$ , respectively. Note that the function  $\rho(t)$  is determined by the spectrum of  $i(t)$ ,  $q(t)$ . Starting with the pdf  $p(i_1, i_2, q_1, q_2)$ , one can calculate the pdf and covariance function of the polar components  $[r_1, r_2, \theta_1, \theta_2]^T$ .

This has been partly done in [6, 7, 8]. Below the covariance functions of  $r(t)$ ,  $\theta(t)$ ,  $m(t)$  are summarized:

P1) The covariance function between  $r_1$  and  $r_2$  is  $c_{rr}(t) = \sigma_r^2 \rho_r(\rho(t))$  where  $\sigma_r^2 = (2 - \frac{\pi}{2})\sigma^2$  is the variance of  $r$  and

$$\rho_r(\rho) = \frac{2E(\rho^2) - (1 - \rho^2)K(\rho^2) - \frac{\pi}{2}}{(2 - \frac{\pi}{2})} \quad (9)$$

$$= \frac{\pi\rho^2}{4(4-\pi)} \sum_{n=0}^{\infty} \left( \frac{(2n-1)!!}{(2n)!!} \right)^2 \frac{1}{(n+1)^2} \rho^{2n} \quad (10)$$

$$= \frac{\pi\rho^2}{4(4-\pi)} \left( 1 + \left( \frac{1}{2} \right)^2 \frac{1}{2^2} \rho^2 + \left( \frac{1 \cdot 3}{2 \cdot 4} \right)^2 \frac{1}{3^2} \rho^4 + \dots \right)$$

is the correlation coefficient between  $r_1$  and  $r_2$ .  $K(\rho^2)$  and  $E(\rho^2)$  are the complete elliptic integral of 1st and 2nd kind, and  $(2n-1)!! = 1 \cdot 3 \cdot \dots \cdot (2n-1)$  and  $(2n)!! = 2 \cdot 4 \cdot \dots \cdot (2n)$  denote double factorials, respectively.

P2) Similarly, the covariance function between  $m_1 = e^{j\theta_1}$  and  $m_2 = e^{j\theta_2}$  is  $c_{mm}(t) = \sigma_m^2 \rho_m(\rho(t))$  with  $\sigma_m^2 = 1$  and

$$\rho_m(\rho) = \frac{E(\rho^2) - (1 - \rho^2)K(\rho^2)}{\rho} \quad (11)$$

$$= \frac{\pi\rho}{4} \sum_{n=0}^{\infty} \left( \frac{(2n-1)!!}{(2n)!!} \right)^2 \frac{1}{n+1} \rho^{2n} \quad (12)$$

$$= \frac{\pi\rho}{4} \left( 1 + \left( \frac{1}{2} \right)^2 \frac{1}{2} \rho^2 + \left( \frac{1 \cdot 3}{2 \cdot 4} \right)^2 \frac{1}{3} \rho^4 + \dots \right)$$

P3) The covariance function between  $\theta_1$  and  $\theta_2$  was unknown and is derived for the first time in this paper in a similar way as in [8]. It is  $c_{\theta\theta}(t) = \sigma_\theta^2 \rho_\theta(\rho(t))$  with  $\sigma_\theta^2 = \frac{\pi^2}{3}$  and

$$\rho_\theta(\rho) = \frac{3\rho}{2\pi} \left( 1 + \frac{1}{2\pi} \rho + \frac{1}{6} \rho^2 + \frac{5}{24\pi} \rho^3 + \dots \right). \quad (13)$$

Computing the Fourier transform of the above covariance functions results in the spectrum of the polar signals  $r(t)$ ,  $m(t)$ ,  $\theta(t)$ :

$$\begin{aligned} C_{rr}(\omega) &= \sigma_r^2 \mathcal{F}(\rho_r(\rho(t))), \\ C_{mm}(\omega) &= \sigma_m^2 \mathcal{F}(\rho_m(\rho(t))), \\ C_{\theta\theta}(\omega) &= \sigma_\theta^2 \mathcal{F}(\rho_\theta(\rho(t))) \end{aligned} \quad (14)$$

where  $\rho(t) = c_{ii}(t)/\sigma^2 = \mathcal{F}^{-1}(C_{ii}(\omega))/\sigma^2$  is determined by the spectrum  $C_{ii}(\omega)$  in the Cartesian domain. By using the power series of  $\rho_r(\rho)$ ,  $\rho_m(\rho)$ ,  $\rho_\theta(\rho)$  in Eq. (10), (12), (13) and the fact that a multiplication in the time domain corresponds to a convolution in the frequency domain, the spectra in the polar domain become

$$\begin{aligned} C_{rr}(\omega) &= \frac{\pi}{8} \sigma^2 \left( \Gamma_2(\omega) + \frac{1}{16} \Gamma_4(\omega) + \dots \right), \\ C_{mm}(\omega) &= \frac{\pi}{4} \left( \Gamma(\omega) + \frac{1}{8} \Gamma_3(\omega) + \dots \right), \\ C_{\theta\theta}(\omega) &= \frac{\pi}{2} \left( \Gamma(\omega) + \frac{1}{2\pi} \Gamma_2(\omega) + \frac{1}{6} \Gamma_3(\omega) + \dots \right). \end{aligned} \quad (15)$$

$\Gamma(\omega) = \mathcal{F}(\rho(t)) = C_{ii}(\omega)/\sigma^2$  is the normalized spectrum in the Cartesian domain and the notation  $\Gamma_k(\omega) = \mathcal{F}(\rho^k(t)) = \Gamma_{k-1}(\omega) * \Gamma(\omega)$  denotes the  $(k-1)$ -times self-convolution of  $\Gamma(\omega)$ . Actually, it is this self-convolution of  $\Gamma(\omega)$  which leads to the spectrum growth in the polar domain.

One interesting question is: If both  $r(t)$  and  $m(t)$  have a wider spectrum, why does the baseband signal  $s(t) = r(t)m(t)$  have a narrow, the originally given spectrum? If  $r(t)$  and  $m(t)$  were independent, the covariance function of  $s(t)$  would be the product of the covariance functions of  $s(t)$  and  $m(t)$ . Then the spectrum of  $s(t)$  being the convolution of their spectra would be even wider. This is fortunately not the case. As  $r(t)$  and  $m(t)$  are highly dependent [8], the spectrum of  $r(t)m(t)$  is not simply the convolution of the spectra of  $r(t)$  and  $m(t)$ . In other words, the polar representation of the baseband signal implies only an *internal* spectral growth inside the polar modulator and does not change the spectrum of the transmitted RF signal in Eq. (3).

Fig. 3 a) shows the normalized spectra of  $i(t)$ ,  $r(t)$ ,  $\theta(t)$ ,  $m(t)$  for a Gaussian pulse shaping filter  $g(t)$  with the time-bandwidth-product  $BT_{\text{sym}} = 0.3$ . As expected, the polar signals have a much wider spectrum than  $i(t)$ . The reason that the phase signals  $\theta(t)$  and  $m(t) = e^{j\theta(t)}$  show a stronger spectral growth than the amplitude  $r(t)$  is that the higher-order self-convolutions in  $C_{\theta\theta}(\omega)$ ,  $C_{mm}(\omega)$  in Eq. (15) decay much slower to zero than in  $C_{rr}(\omega)$ . Fig. 3 b) demonstrates the same behavior for a root-raised-cosine (RRC) pulse shaping filter  $g(t)$  with the roll-off factor  $\beta = 0.5$ .  $C_{ii}(\omega)$  is perfectly bandlimited in this case, but the spectra of the polar signals are not bandlimited.

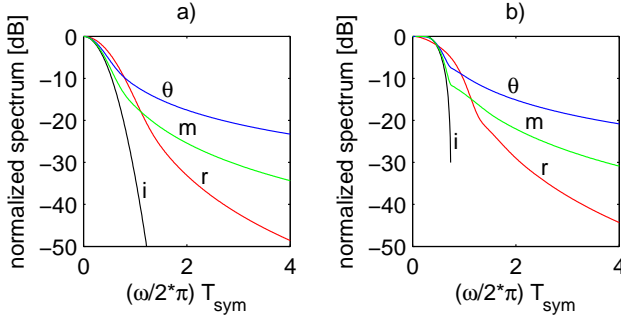


**Fig. 3.** Normalized spectra in the Cartesian and polar domain for a) Gaussian b) RRC pulse shaping filter

## 5. SIMULATIONS

One limitation of the above theoretical study is the use of the simplified signal model in section 3.3. In reality,  $s(t)$  is not perfectly Gaussian. The question is thus: How good are the theoretical results for the practice?

Fig. 4 compares the theoretical results from the previous section with those calculated from simulated data based on the exact signal model in section 3.2. It shows the pdf<sup>1</sup> and normalized spectrum of  $i(t)$ ,  $r(t)$ ,  $\theta(t)$ ,  $m(t)$  for LTE downlink (16-QAM, 2048-point IFFT, equal power in all OFDM carriers). Due to the large IFFT length,  $s(t)$  is almost perfectly Gaussian. The result is a perfect match in both the pdf and spectrum between the theory and simulation. This is also the case when the OFDM carriers have different powers.

<sup>1</sup>Since  $m = e^{j\theta}$  is complex, only the pdf of  $\cos \theta$  is shown.

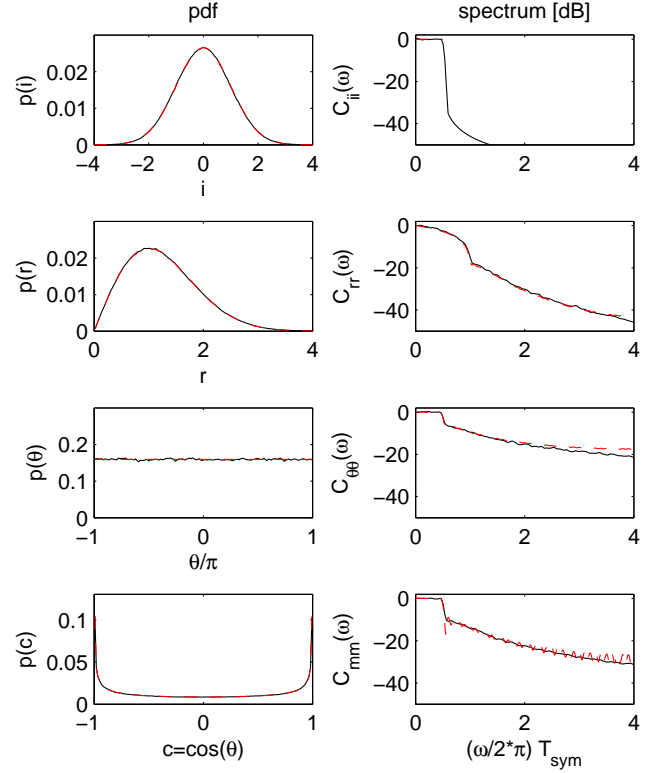


**Fig. 4.** Comparison between theory (---) and simulation (—) for LTE downlink

In another EDGE simulation, a sequence of random 8PSK symbols is filtered by a Gaussian-like pulse shaping filter. Since the EDGE pulse shaping filter is pretty short (roughly 5 symbols) in comparison to the IFFT length in LTE, the filter output  $s(t)$  in EDGE is much less Gaussian. Though the Gaussian assumption is remarkably violated in this case, the agreement in the spectra of polar signals between the theory and simulation is still satisfactory (no plot due to limited space).

## 6. CONCLUSION

The choice of the internal representation of a communication signal inside the modulator has a great impact to its spectral properties. This paper gives an analytic study of the spectral growth in polar transmitters. By assuming a simplified Gaussian signal model, the spectral growth of the polar signals can be predicted for any given spectrum of the IQ signal. Simulations show that the theoretical results agree well with practice even if the Gaussian assumption is sometimes violated.

The choice of the signal representation has also impact on other signal processing issues in communication systems. For example, the effect of a linear filtering or quantization of the polar signals to the spectrum of IQ signal is nontrivial and has also to be investigated.

## 7. REFERENCES

- [1] L. R. Kahn, "Single-sideband transmission by envelope elimination and restoration," *Proc. of IRE*, vol. 40, pp. 803–806, 1952.
- [2] J. Groe, "Polar transmitters for wireless communications," *IEEE Communications Magazine*, vol. 45, pp. 58–63, 2007.
- [3] F. H. Raab, P. Asbeck, et al., "Power amplifiers and transmitters for RF and microwave," *IEEE Trans. Microwave Theory and Techniques*, vol. 50, pp. 814–826, 2002.
- [4] J. Lopez, L. Yan, et al., "Design of highly efficient wide-band RF polar transmitters using the envelope-tracking technique," *IEEE Journal of Solid-State Circuits*, vol. 44, pp. 2276–2294, 2009.
- [5] J. Zhuang, K. Waheed, and R. B. Staszewski, "A technique to reduce phase/frequency modulation bandwidth in a polar RF transmitter," *IEEE Trans. Circuits and Systems*, vol. 57, pp. 2196–2207, 2010.
- [6] D. K. C. MacDonald, "Some statistical properties of random noise," *Proc. Cambridge Philosophical Society*, vol. 45, pp. 368–372, 1949.
- [7] R. Price, "A note on the envelope and phase-modulated components of narrow-band Gaussian noise," *IRE Trans. on Information Theory*, vol. 1, pp. 9–13, 1955.
- [8] M. Ibrahim and B. Yang "A theoretical study of the statistical and spectral properties of polar transmitter signals," *Proc. ISCAS*, pp. 1512–1515, 2014.
- [9] J. E. Volder, "The CORDIC trigonometric computing technique," *IRE Trans. Electronic Computers*, vol. 8, pp. 330–334, 1959.
- [10] J. S. Walther, "A unified algorithm for elementary functions," in *Spring Joint Computer Conference*, 1971, pp. 379–385.
- [11] J. G. Proakis, *Digital Communications*, McGraw-Hill, 4 edition, 2000.
- [12] A. Papoulis and S. U. Pillai, *Probability, Random Variables and Stochastic Process*, McGraw-Hill, 4 edition, 2002.